Biochemical and Biophysical Research Communications 462 (2015) 46–51

Contents lists available at ScienceDirect

Biochemical and Biophysical Research Communications

journal homepage: www.elsevier.com/locate/ybbrc

The structure and conformational switching of Rap1B

Hiroki Noguchi [a], Takahisa Ikegami [a], Aritaka Nagadoi [a], Yuji O. Kamatari [b], Sam-Yong Park [a], Jeremy R.H. Tame [a, *], Satoru Unzai [a, *]

[a] Graduate School of Medical Life Science, Yokohama City University, 1-7-29 Suehiro, Yokohama, Kanagawa 230-0045, Japan
[b] Life Science Research Center, Gifu University, Gifu 501-1194, Japan

ARTICLE INFO

Article history:
Received 10 April 2015
Available online 29 April 2015

Keywords:
G protein
Protein crystallography
Mutant
Conformation change
Rap1

ABSTRACT

Rap1B is a small GTPase involved in the regulation of numerous cellular processes including synaptic plasticity, one of the bases of memory. Like other members of the Ras family, the active GTP-bound form of Rap1B can bind to a large number of effector proteins and so transmit signals to downstream components of the signaling pathways. The structure of Rap1B bound only to a nucleotide has yet to be solved, but might help reveal an inactive conformation that can be stabilized by a small molecule drug. Unlike other Ras family proteins such as H-Ras and Rap2A, Rap1B crystallizes in an intermediate state when bound to a non-hydrolyzable GTP analog. Comparison with H-Ras and Rap2A reveals conservative mutations relative to Rap1B, distant from the bound nucleotide, which control how readily the protein may adopt the fully activated form in the presence of GTP. High resolution crystallographic structures of mutant proteins show how these changes may influence the hydrogen bonding patterns of the key switch residues.

1. Introduction

Ras-related protein 1 (Rap1) exists as two 95% identical isoforms A and B that play a number of crucial roles in regulating cell adhesion, cell junction formation, cell secretion, and cell polarity [1], but with quantifiable differences in localization and function [2]. Rap1 is a member of the small GTPase family that includes proteins such as H-Ras, K-Ras and M-Ras [3]. These proteins act as molecular switches by cycling between an inactive GDP-bound form and an active GTP-bound form [4,5]. They are involved in many cellular signal transduction pathways, controlling cell growth, migration and proliferation. Guanine nucleotide exchange factors (GEFs) catalyze the dissociation of GDP and binding of GTP, and GTPase activating proteins (GAPs) accelerate the GTP hydrolysis reaction, so that signaling is up- and down-regulated by these factors [6].

Previous analyses of H-Ras and M-Ras revealed that the majority of the structure is relatively invariant on replacing GDP with GTP, but two loop regions undergo substantial conformational changes [6–9]. These loop regions are called switch I and switch II, which are localized in-between a β strand and an α helix (either β2 or β3 and α1), close to the nucleotide binding site. The presence of a γ-phosphate group on the bound nucleotide and attendant magnesium ion is detected by the switch I and switch II regions forming bonds with them, creating a binding surface recognized by effector proteins. However, the GTP-bound GTPases may adopt two states, called state-1 and state-2, respectively. State-2 is defined by coordination of the magnesium ion by a conserved threonine side-chain in the switch I region (Thr-35 in Rap1B), and represents the activated form.

Different Ras family members show very different conformational preferences in the GppNHp bound form, with the state-2/state-1 ratio ranging from 0.072 for M-Ras to 16 for Rap2A [10,11], despite sharing an identical switch I sequence (YDPTIED). M-Ras shows the greatest tendency to adopt state-1 with GppNHp bound, leaving a spacious hydrophobic pocket near the nucleotide [12]. Small molecule Ras inhibitors have been developed by targeting this pocket, and there are hopes this may prove a generally useful strategy for inhibiting Ras signaling [13,14]. Since Rap1B is associated with several types of cancer, there is a strong interest in developing specific drugs that can down-regulate Rap1B signaling. Although the crystal structures are known of several complexes formed by Rap1B and effector proteins, no models are published of Rap1B in the presence of nucleotides alone. We have therefore

Abbreviations: GppNHp, guanosine 5′[β,γ-imido]triphosphate.

* Corresponding authors. Fax: +81 45 508 7366.
E-mail addresses: jtame@tsurumi.yokohama-cu.ac.jp (J.R.H. Tame), unzai@tsurumi.yokohama-cu.ac.jp (S. Unzai).

http://dx.doi.org/10.1016/j.bbrc.2015.04.103

determined high resolution crystal structures of rat Rap1B (wild-type and mutants) bound only to GDP or GppNHp, to clarify the mechanism of activation and assist drug design.

2. Materials and methods

2.1. Cloning

The rat Rap1B gene (Uniprot Q62636, residues 1–167) was amplified from a cDNA library of adult rat brain (GenoStaff) by PCR and cloned into the pET21b expression vector (Novagen), between the *Nde*I and *Not*I restriction sites. The gene was amplified by using the following pairs of primers:

5′-CGGGAATTCCATATGCGTGAATATAAGCTAGTCGTTC-3′ (*Nde*I site underlined)
5′-TTTTCCTTTTGCGGCCGCTTATCTGTTAATTTGCCGCACTAGG-3′ (*Not*I site underlined)

2.2. Expression and purification

The pET21b/Rap1B (residues 1–167) plasmid was transformed into *Escherichia coli* BL21 (DE3) cells including a pGro7 chaperone vector (Takara). Cells were grown at 37 °C in LB medium (containing 50 μg/ml ampicillin, 20 μg/ml chloramphenicol, and 2 mg/ml L-Arabinose) up to OD_{600} of 0.8. Protein expression was induced by adding isopropyl β-D-1-thiogalactopyranoside (IPTG) to a final concentration of 0.5 mM and shaking overnight at 22 °C. Rap1B was purified using Q-Fast flow (GE Healthcare) and HiLoad 16/600 Superdex 200 columns (GE Healthcare).

2.3. Nucleotide exchange

Rap1B-GDP was prepared by incubating purified Rap1B in the presence of rat SynGAP C2-GAP domain (Uniprot ID Q9QUH6, residues 237–714) and 1 mM GDP (Nacalai tesque) overnight at 4 °C in 20 mM Tris–HCl (pH 8.0), 300 mM NaCl, 5 mM $MgCl_2$, and 1 mM DTT. Phosphate and SynGAP C2-GAP domain were removed by gel filtration. Rap1B-GppNHp (wild-type and mutants) were prepared as described [15].

2.4. Crystallization of Rap1B-GppNHp and Rap1B-GDP

Rap1B-GppNHp (10 mg/ml) and Rap1B-GDP (10 mg/ml) were dialyzed against 20 mM HEPES pH 7.4, 50 mM NaCl, and 5 mM $MgCl_2$. The wild-type and L9V mutant Rap1B-GppNHp crystals were obtained by hanging drop vapor diffusion method using a reservoir solution containing 0.1 M HEPES pH 7.5, 12% (w/v) PEG3350, and 5 mM $CdCl_2$ at 20 °C. Crystals of wild-type Rap1B-GDP were grown by same method using the reservoir solution containing 0.1 M Li_2SO_4, 0.1 M Tris–HCl pH 8.5, 30% (w/v) PEG4000, and 1 mM $CdCl_2$. The Rap1B(T65A)-GppNHp crystals were obtained by hanging drop vapor diffusion using a reservoir solution containing 0.2 M Li_2SO_4, 0.1 M bis-Tris pH 5.5, and 25% (w/v) PEG3350 at 20 °C.

2.5. Data collection and structure determination

All X-ray diffraction data were collected at beam-line 17A of the Photon Factory (Tsukuba, Japan) using an ADSC Quantum 270 CCD detector or DECTRIS PILATUS-3S 6M detector. Diffraction data were processed with HKL2000 [16] or iMOSFLM [17]. General data handling was carried out with the CCP4 suite [18]. The crystal structure of Rap1B-GppNHp was determined by molecular replacement with the program MOLREP [19] using a Ras-GppNHp structure (PDB entry 5P21). Further models were solved by bootstrapping from this Rap1B model. The models were manipulated with COOT [20]. Refinement was carried out with PHENIX [21]. The final structures were validated with MolProbity [22]. Data collection and refinement statistics are shown in Table 1.

2.6. Accession numbers

The models have been deposited in the Research Collaboratory for Structural Bioinformatics Protein Data Bank (PDB) with accession codes 3X1W (Rap1B-GDP), 3X1X (Rap1B-GppNHp), 3X1Y (Rap1B(L9V)-GppNHp) and 3X1Z (Rap1B(T65A)-GppNHp).

3. Results

Rat Rap1B has an N-terminal catalytic domain of 167 residues, identical to the human protein, except that Cys 139 (human) is replaced by serine (rat); this surface residue is over 20 Å from the bound nucleotide and has no appreciable effect on the structure. The catalytic domain of rat Rap1B was chosen for analysis because it contains fewer cysteine residues that may accidentally form disulfide bonds. Within the N-terminal domain, human Rap1A and Rap1B differ at only three positions, Cys 48→Ala, Glu 107→Asp, and Cys 139→Asn. A sequence alignment of Rap1B and H-Ras is given in Fig. 1A, and the structure of the catalytic domain is shown in Fig. 1B.

3.1. Comparison of the native GDP and GppNHp complexes

Very high resolution X-ray diffraction data were collected for both Rap1B complexes, and a summary of the refinement statistics is provided in Table 1. The catalytic domain of the Ras family consists of a central β-sheet (β1-β6) with five α-helices (α1-α5) and ten loops, (L1-L10) [23]. Comparing Rap1B with other Ras family catalytic domains, the rmsd values of the Cα atoms are in the region of 1.2 Å. L1 is known as the phosphate binding loop (P loop), and consists of residues 10-17 in Rap1. The P loop interacts with the bound nucleotide but its conformation is the same in both the GDP and GTP bound forms. Ser 17 coordinates the Mg^{2+} ion. The GDP and GppNHp complexes were both crystallized in space-group $P2_12_12_1$ with very similar cell parameters and a single molecule in the asymmetric unit. Switch I, residues 32-38, is a loop found between α1 and β2. Switch II, residues 60-70, forms half of L5 and half of α2. Representative electron density maps covering the ligands for the GDP and GppNHp complexes are shown in Fig. 2A and B respectively.

In the GppNHp complex, the switch I and II regions form a mutual crystallographic contact, with the main-chain nitrogen atoms of Thr 35 and Ile 36 of one molecule making hydrogen bonds to the side-chain oxygen atom of *Asn 74* of a neighbor. (Residue names of neighboring molecules are shown in italics.) The side-chain of Thr 35 points away from the nucleotide, and lies close to the side-chain of *Lys 5*. Tyr 32 also contacts *Tyr 71*. The electron density map is very clear in this region and shows both switch I and switch II to be well ordered, but separated from the GppNHp by a number of water molecules hydrating the phosphate groups (Fig. 2B). The crystal contact formed by the switch regions is significantly smaller in the GDP bound form; Thr 35 no longer makes any contact with the neighboring molecule, and *Asn 74* makes a hydrogen bond to the carbonyl oxygen of Pro 34. In both structures the Mg^{2+} ion is coordinated by a water molecule in place of Thr 35 (Fig. 2A and B). Although the crystal contacts may influence the conformations of switch I and switch II in the structures described here, differences between the two crystal forms show that the phosphate groups of the nucleotide ligand still exercise

Table 1
Data collection and refinement statistics. Values in parentheses are for the outer shell.

	Rap1B(Wild) -GppNHp	Rap1B(Wild) -GDP	Rap1B(L9V) -GppNHp	Rap1B(T65A) -GppNHp
Data collection				
Resolution range (Å)	50.0–1.00 (1.02–1.00)	50.0–1.20 (1.22–1.20)	35.42–1.17 (1.19–1.17)	33.96–1.25 (1.27–1.25)
Space group	$P2_12_12_1$	$P2_12_12_1$	$P2_12_12_1$	$P2_1$
Unit-cell parameters				
a (Å)	43.72	43.52	43.60	37.42
b (Å)	52.46	52.43	52.60	59.04
c (Å)	60.79	60.55	60.72	68.07
α (°)	90.00	90.00	90.00	90.00
β (°)	90.00	90.00	90.00	93.68
γ (°)	90.00	90.00	90.00	90.00
No. of measured reflections	421,896	150,480	413,294	344,135
No. of unique reflections	71,678	41,776	47,011	78,079
Completeness (%)	93.9 (92.3)	94.7 (87.1)	98.0 (93.3)	95.5 (92.7)
Mean I/σ (I)	38.3 (5.1)	27.3 (2.5)	23.3 (8.9)	12.5 (3.0)
Multiplicity	5.9 (5.8)	3.7 (2.2)	8.8 (7.0)	4.4 (4.2)
R_{merge}[a] (%)	7.0 (53.2)	5.5 (34.9)	4.7 (16.7)	5.1 (43.3)
Refinement statistics				
Resolution range (Å)	18.90–1.00	24.85–1.20	35.42–1.17	33.96–1.25
R factor[b] (%)	19.6	19.5	17.6	14.6
R_{free}[b] (%)	21.1	22.4	21.9	17.2
Solvent molecules	152	72	193	354
R.m.s. deviations from ideal				
Bond lengths (Å)	0.006	0.007	0.009	0.007
Bond angles (°)	1.265	1.171	1.477	1.240
Chiral volumes (Å^3)	0.078	0.080	0.102	0.044
Ramachandran plot, residues in (%)				
Most favourable region	98.78	97.58	98.18	97.27
Additional allowed region	1.22	1.82	1.82	2.73

[a] $R_{merge} = \sum_{hkl}\sum_i |I_i(hkl) - \langle I(hkl)\rangle| / \sum_{hkl}\sum_i I_i(hkl)$, where $I_i(hkl)$ is the intensity of an observation, $\langle I(hkl)\rangle$ is the mean value for that reflection and the summations are over all reflections.

[b] R factor $= \sum_{hkl} ||F_{obs}| - |F_{calc}|| / \sum_{hkl} |F_{obs}|$, where F_{obs} and F_{calc} are the observed and calculated structure-factor amplitudes, respectively. The free R factor was calculated with 5% of the data excluded from the refinement.

significant control over these surface loops. Comparing the GppNHp and GDP complexes, it can be seen that the loss of the γ-phosphate allows Thr 35 to flip to a position pointing more directly toward the nucleotide; the GDP complex is therefore unexpectedly closer to the active state-2 conformation than Rap1B-GppNHp. Arg 68 forms a salt bridge with Glu 37 in the GDP complex (Fig. 3A), but with GppNHp present the arginine side-chain breaks this bond (Fig. 3B), apparently sensing the electrostatic pull of the γ-phosphate through the peptide bond formed by Ala 59 and Gly 60, part of the conserved DXXG motif of L4 at the start of switch II. Arg 68 hydrogen bonds to the carbonyl oxygen of Ala 59, at the start of switch II, in both structures, but in the GppNHp complex a water molecule is interposed between Arg 68 and Glu 37. The catalytic glutamine side-chain (Gln 63) forms hydrogen bonds to water molecules binding the γ-phosphate, and moves less than 1 Å away from GDP. The movements of Arg 68 and Gln 63 seem to trigger a much larger movement of Phe 64, the benzene ring moving approximately 7 Å to a much more exposed position in the GDP form (Fig. 3A). The close crystal contacts around the switch II region may have favored the observed conformation, but this effect is not

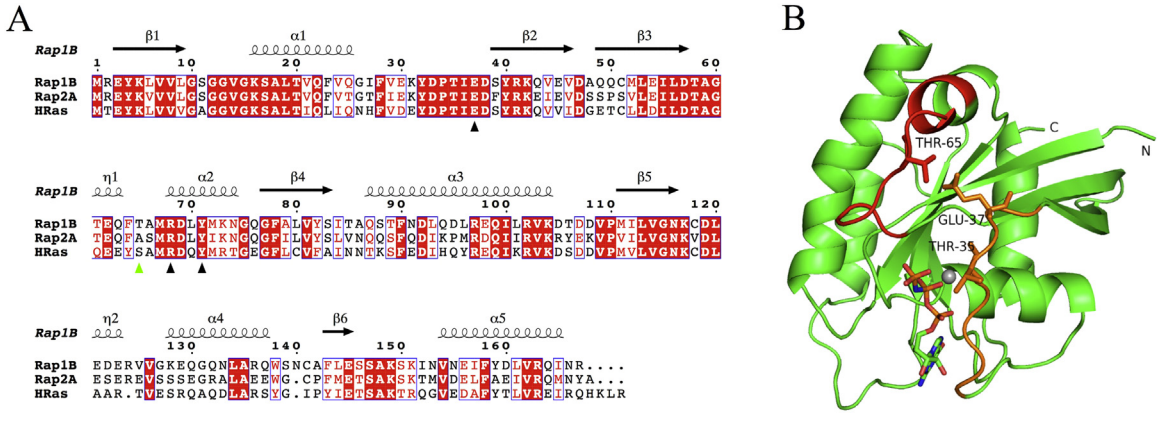

Fig. 1. A) A sequence alignment of rat Rap1B with Rap2A and H-Ras, showing the secondary structure elements of Rap1B. Residues common to the three sequences are shown in white on red, similar residues are shown in red. Black triangles indicate the residues of switch I and switch II whose hydrogen bonding pattern reflects the bound nucleotide and conformational state. A green triangle indicates residue 65, which is notably different in the three proteins. This figure was made with ESPRIPT [26]. B) The overall Cα trace of wild-type rat Rap1B bound to GppNHp, determined in this work. Switch I is shown in orange, and switch II in red. The nucleotide analog is shown as a stick model, and the magnesium ion is shown as a gray sphere. Molecular figures were made with PYMOL [27]. (For interpretation of the references to color in this figure legend, the reader is referred to the web version of this article.)

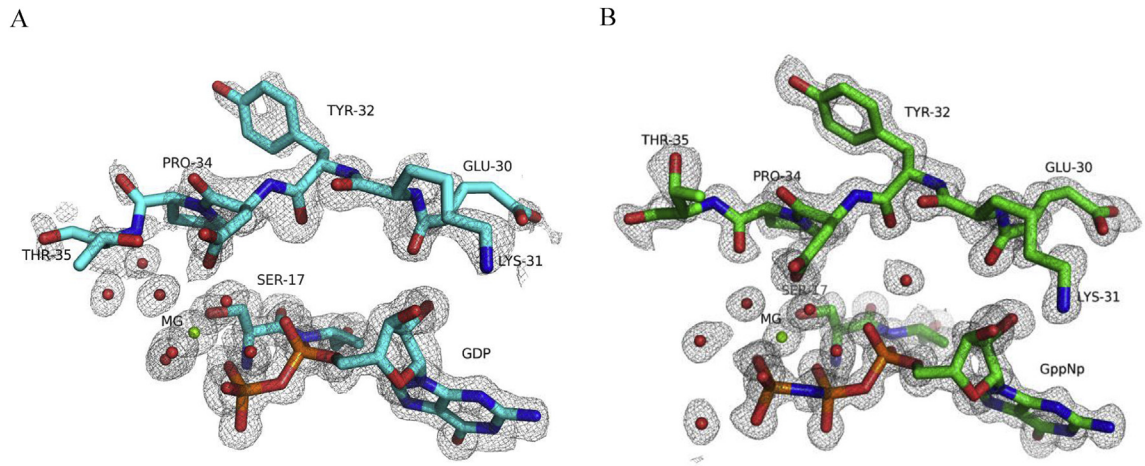

Fig. 2. A) The 2mF_o-DF_c electron density map covering the GDP and switch I region of wild-type Rap1B. Carbon atoms are shown in cyan, oxygen red, nitrogen blue, and phosphorus orange. Water molecules and the magnesium ion are shown as spheres. The electron density is contoured at 1 σ. B) An equivalent view to (A), but showing the GppNHp complex. The color scheme is the same as (A), except that carbon atoms are shown in green. The switch I region is less mobile and better represented in the electron density map than with GDP present. Thr 35 shows a different position, but remains far from the magnesium ion to which it coordinates in the activated state-2 conformation. (For interpretation of the references to color in this figure legend, the reader is referred to the web version of this article.)

unique to studies of Rap1B. In crystal structures of Ral-GppNHp, the switch regions were found to show conformational dependence on crystal contacts, but Nicely and colleagues also observed that different crystal forms of the Ral-GDP complex showed identical switch conformations regardless of the crystal contacts [24], indicating that crystallization is not a dominant factor in determining these loop positions. In fact it was proposed that the crystal contacts may be mimicking a true protein–protein interaction relevant to Ral function *in vivo*.

3.2. Comparison with other Ras proteins

To try to understand why the crystal structure of Rap1B-GppNHp does not show the activated state-2 conformation, we compared the model with other GTPases. One common feature of the GDP and GppNHp complexes of Rap1B is the set of contacts formed by Glu 37 in switch I (Fig. 3A and B). The carboxyl group forms hydrogen bonds with the side-chains of Thr 65 and Tyr 71, and the main-chain nitrogen atom of Ala 59. This position of Glu 37 is incompatible with the state-2 conformation of Thr 35. Although M-Ras has rather different residues and conformation in this region, Glu 37 still forms a hydrogen bond (with Ser 75) that is incompatible with state-2. H-Ras however has no side-chain at a position equivalent to Thr 65 of Rap1B capable of hydrogen bonding to Glu 37. This probably explains the fact that switch II is more ordered in the Rap1B crystal structure than in H-Ras models (with alanine at position 65), and H-Ras shows a stronger tendency to form state-2.

The conserved residue Tyr 71 is found to adopt two rotamers in Ras GTPase proteins, one facing an internal pocket and the other,

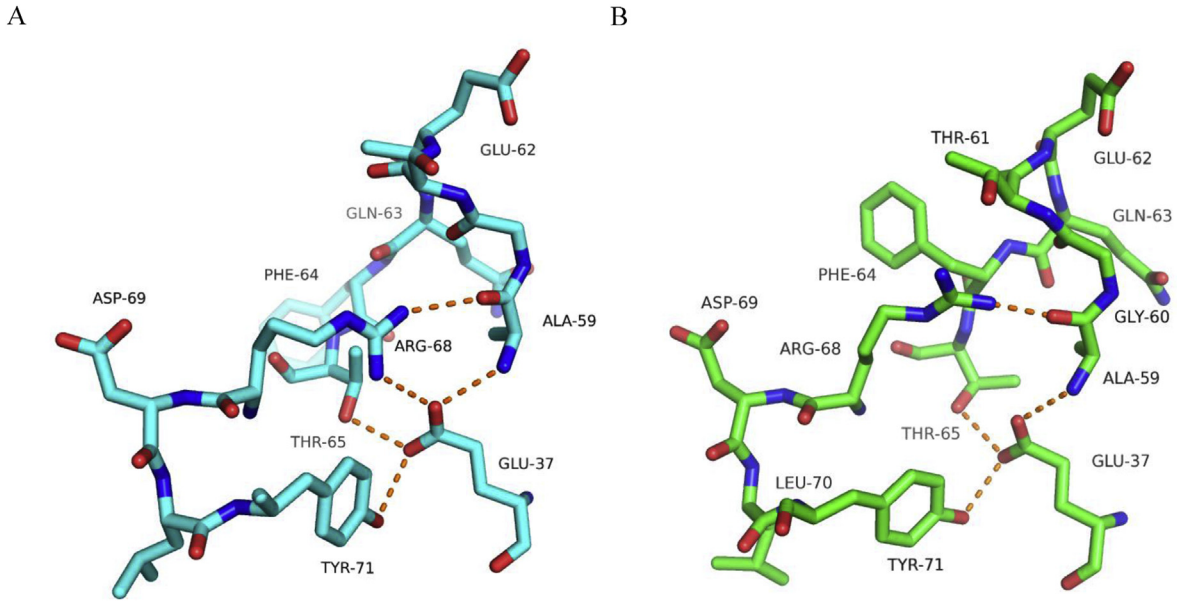

Fig. 3. A) The interaction network around Glu 37 in Rap1B-GDP. The color scheme is that of Fig. 2A, and the salt bridge, hydrogen bonds formed by the Glu 37 and Arg 68 side-chains are shown as dotted orange lines. B) The hydrogen bond network around Glu 37 in Rap1B-GppNHp. Gln 63, Phe 64 and Arg 68 adopt significantly different conformations from the GDP-bound model, despite the similarity of the crystallization conditions and overall crystal packing. Glu 37 retains hydrogen bonds to the Thr 65 and Tyr 71 side-chains, characteristic of the state-1 conformation. (For interpretation of the references to color in this figure legend, the reader is referred to the web version of this article.)

outward-pointing rotamer forms a hydrogen bond with Glu 37. The latter rotamer of Tyr 71 holds Glu 37 away from the activated state-2 conformation. The internal pocket is lined by Val 9 in H-Ras, allowing room for the tyrosine to enter freely. Rap1 has a leucine residue at position 9, which favors the external tyrosine rotamer and the state-1 conformation. Leu 9 of Rap1 is small enough to accommodate Tyr 71 in this internal pocket on switching to state-2, but these internal, conservative mutations also seem to play a role in the delicate balance of conformational preferences of the switch regions through indirect side-chain interactions. Overall our crystal structures suggest Glu 37 plays a significant role in conformation switching, and bound GTP makes the state-2 conformation more accessible by breaking the Glu37-Arg68 salt bridge.

The Rap2A-GTP complex (PDB 3RAP) is the most similar model in PDB to Rap1B-GTP [25], but despite the almost perfect conservation of switch I and switch II, the models show marked differences. Rap2A adopts a state-2 conformation, with the GTP γ-phosphate bonding to the side-chain of Tyr 32, and Thr 35 coordinating the Mg^{2+} ion. In Rap1B-GppNHp, Tyr 32 points to the solvent, while Thr 35 is found more than 5 Å from the nucleotide (Fig. 2B). Like Rap1B, Rap2A has a leucine residue at position 9, favoring state-1 as described above, and Tyr 71 occupies a similar position; but Rap2A also has an alanine residue in place of Thr 65. This threonine side-chain forms a hydrogen bond to Glu 37 in both the Rap1B-GDP and Rap1B-GppNHp structures (Fig. 3A and B). The T65A replacement in Rap2 appears to help shift the conformational preference by loss of the bond to Glu 37, since most amino acid changes between Rap1 and Rap2 occur at surface loops and have little effect on the nearby structure.

3.3. *Mutant Rap1B-GppNHp complexes*

To test the idea that the differences between Rap1B, Rap2A and H-Ras at residues 9 and 65 influence the ease of activation, Rap1B L9V and T65A mutants were prepared and crystallized. For Rap1B(L9V), the electron density map shows some evidence that the smaller valine residue at position 9 does allow Tyr 71 to adopt the activated state more readily (Fig. 4A). Two alternative rotamers of this tyrosine are found in the L9V mutant, corresponding to state-1 and state-2. The principal rotamer however is the one seen in the native structure, so the L9V mutation alone does not give an activated crystal structure.

The T65A mutation has a more marked effect than the L9V replacement, moving the Tyr 71 side-chain, and the switch I and II regions, completely to the state-2 position and breaking its bond to Glu 37 (Fig. 4B). Thr 35 of Rap1B(T65A) coordinates the Mg^{2+} ion in exactly the same way as in Rap2A with a GTP analog present. Residues 9 and 65 therefore both play roles in controlling the conformation of the protein once GTP has bound, through direct or indirect effects on bonds formed by Glu 37.

4. Discussion

The interactions of small GTPases with up- and down-stream partner proteins are controlled by a number of factors that allow a complex interplay between different pathways. The functional and conformational flexibility of two small surface loops provides sufficient variability and commonality for both unique and shared partners, each binding with appropriate affinity. Questions remain however as to how the conserved switch I region allows the observed multitude of specific partner interactions, and clearly residues outside the immediate binding sites also play significant roles in regulating interactions. We have solved the structure of Rap1B bound to GDP and GppNHp, showing minor changes around the switch I region when GDP is replaced with GppNHp. Although the switch regions are at crystal contacts in the X-ray models described here, crystallization in a state-1 form would not be possible if this structure were not thermodynamically accessible, even with GppNHp bound. The crystal structures of the L9V and T65A mutants demonstrate how conservative mutations may help control the balance between active and inactive structures among Ras proteins generally.

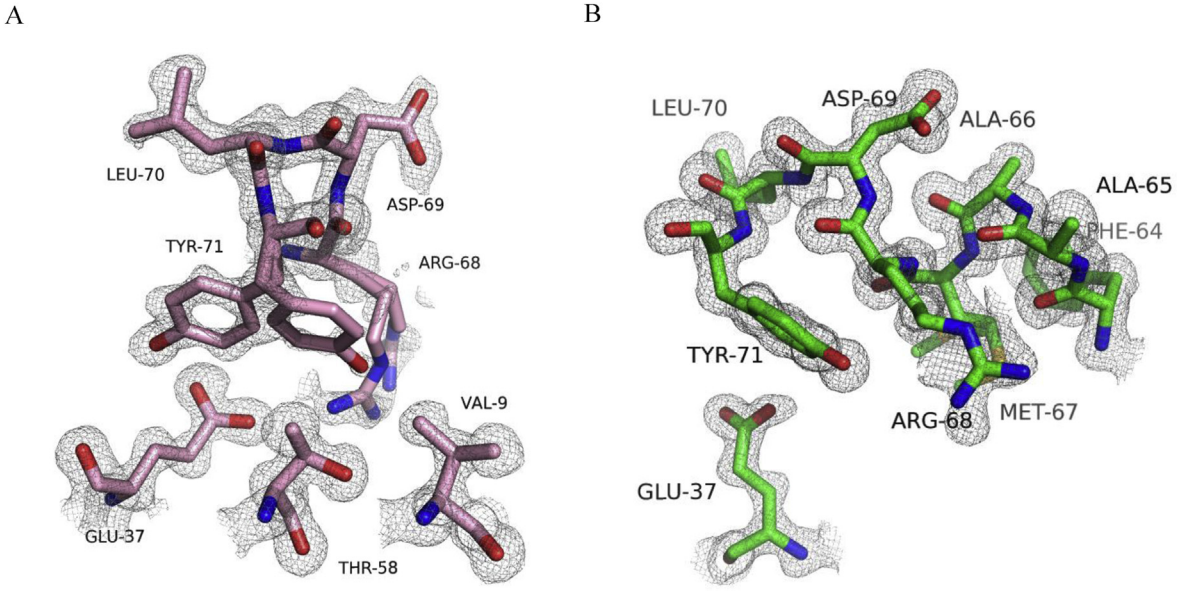

Fig. 4. A) The $2mF_o$-DF_c electron density map of the L9V Rap1B mutant. Reducing the residue size at position 9 allows Tyr 71 more easily to adopt the rotamer found in the activated state-2 conformation. The map indicates that the major conformation is the same as that of wild-type (state-1), but the size of residue 9 controls the balance between these forms. B) The $2mF_o$-DF_c electron density map of the T65A Rap1B mutant. Loss of the hydrogen bond between residues 65 and 37 also breaks the Glu37-Tyr 71 hydrogen bond and switches the protein to the state-2 conformation, with Thr 35 coordinating the magnesium ion. The switch I and II regions are well ordered in the electron density map, clearly showing the truncated side-chain at residue 65.

Conflict of interest

None.

Acknowledgments

We thank Drs. Noboru Komiyama, Hidekazu Hiroaki, Gloria Fuentes and Arnout Voet for their helpful suggestions, Prof. Satoko Akashi for electrospray mass spectrometry measurements, Dr. Hisashi Yoshida for help with X-ray data collection. We thank the Photon Factory staff for their kind assistance. This work was supported by Grant-in-Aid for Scientific Research to S.U. from the Japan Society for the Promotion of Science (JSPS Grant Number 23570145 and 15K06980).

Transparency document

Transparency document related to this article can be found online at http://dx.doi.org/10.1016/j.bbrc.2015.04.103.

References

[1] J.H. Raaijmakers, J.L. Bos, Specificity in Ras and Rap signaling, J. Biol. Chem. 284 (2009) 10995–10999.
[2] E.S. Wittchen, A. Aghajanian, K. Burridge, Isoform-specific differences between Rap1A and Rap1B GTPases in the formation of endothelial cell junctions, Small GTPases 2 (2011) 65–76.
[3] W.J. Pannekoek, M.R. Kooistra, F.J. Zwartkruis, J.L. Bos, Cell-cell junction formation: the role of Rap1 and Rap1 guanine nucleotide exchange factors, Biochim. Biophys. Acta 1788 (2009) 790–796.
[4] H.R. Bourne, D.A. Sanders, F. McCormick, The GTPase superfamily: a conserved switch for diverse cell functions, Nature 348 (1990) 125–132.
[5] H.R. Bourne, D.A. Sanders, F. McCormick, The GTPase superfamily: conserved structure and molecular mechanism, Nature 349 (1991) 117–127.
[6] J. Cherfils, M. Zeghouf, Regulation of small GTPases by GEFs, GAPs, and GDIs, Physiol. Rev. 93 (2013) 269–309.
[7] A.E. Karnoub, R.A. Weinberg, Ras oncogenes: split personalities, Nat. Rev. Mol. Cell. Biol. 9 (2008) 517–531.
[8] N. Mitin, K.L. Rossman, C.J. Der, Signaling interplay in Ras superfamily function, Curr. Biol. 15 (2005) R563–R574.
[9] I.R. Vetter, A. Wittinghofer, The guanine nucleotide-binding switch in three dimensions, Science 294 (2001) 1299–1304.
[10] R.B. Fenwick, S. Prasannan, L.J. Campbell, D. Nietlispach, K.A. Evetts, J. Camonis, H.R. Mott, D. Owen, Solution structure and dynamics of the small GTPase RalB in its active conformation: significance for effector protein binding, Biochemistry 48 (2009) 2192–2206.
[11] J. Liao, F. Shima, M. Araki, M. Ye, S. Muraoka, T. Sugimoto, M. Kawamura, N. Yamamoto, A. Tamura, T. Kataoka, Two conformational states of Ras GTPase exhibit differential GTP-binding kinetics, Biochem. Biophys. Res. Commun. 369 (2008) 327–332.
[12] M. Ye, F. Shima, S. Muraoka, J. Liao, H. Okamoto, M. Yamamoto, A. Tamura, N. Yagi, T. Ueki, T. Kataoka, Crystal structure of M-Ras reveals a GTP-bound "off" state conformation of Ras family small GTPases, J. Biol. Chem. 280 (2005) 31267–31275.
[13] J.M. Ostrem, U. Peters, M.L. Sos, J.A. Wells, K.M. Shokat, K-Ras(G12C) inhibitors allosterically control GTP affinity and effector interactions, Nature 503 (2013) 548–551.
[14] F. Shima, Y. Yoshikawa, M. Ye, M. Araki, S. Matsumoto, J. Liao, L. Hu, T. Sugimoto, Y. Ijiri, A. Takeda, Y. Nishiyama, C. Sato, S. Muraoka, A. Tamura, T. Osoda, K. Tsuda, T. Miyakawa, H. Fukunishi, J. Shimada, T. Kumasaka, M. Yamamoto, T. Kataoka, In silico discovery of small-molecule Ras inhibitors that display antitumor activity by blocking the Ras-effector interaction, Proc. Natl. Acad. Sci. U. S. A. 110 (2013) 8182–8187.
[15] J. John, R. Sohmen, J. Feuerstein, R. Linke, A. Wittinghofer, R.S. Goody, Kinetics of interaction of nucleotides with nucleotide-free H-ras p21, Biochemistry 29 (1990) 6058–6065.
[16] Z. Otwinowski, W. Minor, Meth Enzymol. 276 (1997) 307–326.
[17] T.G. Battye, L. Kontogiannis, O. Johnson, H.R. Powell, A.G. Leslie, iMOSFLM: a new graphical interface for diffraction-image processing with MOSFLM, Acta Crystallogr. D. Biol. Crystallogr. 67 (2011) 271–281.
[18] CCP4, Acta Crystallogr. D. Biol. Crystallogr. 50 (1994) 760–763.
[19] A. Vagin, A. Teplyakov, An approach to multi-copy search in molecular replacement, Acta Crystallogr. D. Biol. Crystallogr. 56 (2000) 1622–1624.
[20] P. Emsley, K. Cowtan, Coot: model-building tools for molecular graphics, Acta Crystallogr. D. Biol. Crystallogr. 60 (2004) 2126–2132.
[21] P.D. Adams, P.V. Afonine, G. Bunkoczi, V.B. Chen, I.W. Davis, N. Echols, J.J. Headd, L.W. Hung, G.J. Kapral, R.W. Grosse-Kunstleve, A.J. McCoy, N.W. Moriarty, R. Oeffner, R.J. Read, D.C. Richardson, J.S. Richardson, T.C. Terwilliger, P.H. Zwart, PHENIX: a comprehensive Python-based system for macromolecular structure solution, Acta Crystallogr. D. Biol. Crystallogr. 66 (2010) 213–221.
[22] V.B. Chen, W.B. Arendall 3rd, J.J. Headd, D.A. Keedy, R.M. Immormino, G.J. Kapral, L.W. Murray, J.S. Richardson, D.C. Richardson, MolProbity: all-atom structure validation for macromolecular crystallography, Acta Crystallogr. D. Biol. Crystallogr. 66 (2010) 12–21.
[23] M.V. Milburn, L. Tong, A.M. deVos, A. Brunger, Z. Yamaizumi, S. Nishimura, S.H. Kim, Molecular switch for signal transduction: structural differences between active and inactive forms of protooncogenic ras proteins, Science 247 (1990) 939–945.
[24] N.I. Nicely, J. Kosak, V. de Serrano, C. Mattos, Crystal structures of Ral-GppNHp and Ral-GDP reveal two binding sites that are also present in Ras and Rap, Structure 12 (2004) 2025–2036.
[25] J. Cherfils, J. Menetrey, G. Le Bras, I. Janoueix-Lerosey, J. de Gunzburg, J.R. Garel, I. Auzat, Crystal structures of the small G protein Rap2A in complex with its substrate GTP, with GDP and with GTPgammaS, Embo J. 16 (1997) 5582–5591.
[26] P. Gouet, E. Courcelle, D.I. Stuart, F. Metoz, ESPript: multiple sequence alignments in PostScript, Bioinformatics 15 (1999) 305–308.
[27] W.L. DeLano, The PyMOL Molecular Graphics System, DeLano Scientific, San Carlos, CA, 2002.